A Three Dimensional Fluid-Structure Interaction Finite Element Model of Wave Propagation in SAW Device: Application to Bio-fouling Removal

Reetu Singh, Subramanian K.R.S. Sankaranarayanan, and Venkat R. Bhethanabotla *
Sensors Research Laboratory, Department of Chemical and Biomedical Engineering,
University of South Florida, Tampa, Florida, 33620, USA.

Abstract

Non-specific protein binding to the surface acoustic wave (SAW) device surfaces, during bio-sensing applications, leads to bio-fouling which causes a significant reduction in their sensitivity and selectivity thereby posing a major challenge to the biosensing applications of SAW devices. A potential technique to remove the non-specifically bound proteins from the device surface is SAW induced acoustic streaming, which results from fluid motion induced from high intensity sound waves. Understanding the fluid-device interaction is critical to efficiently utilize acoustic streaming for biofouling removal to increase device selectivity and sensitivity.

In this work, we have developed, for the first time, a three dimensional coupled field finite element fluid-structure interaction model of a SAW device subject to a liquid loading, to perform investigations into the SAW induced acoustic streaming phenomenon. The wave propagation and the generated velocity fields/profiles are analyzed and their implications for biofouling removal are discussed. Our results indicate that the normal component of fluid velocity is smaller than the tangential component along the propagation direction. Thus, the SAW induced drag force, arising from the tangential component of fluid velocity and leading to particle advection is an important mechanism in biofouling removal from the SAW device surface and the normal component would prevent the reattachment of the particles to the device surface.

I. Introduction

Surface acoustic wave (SAW) sensors find a wide range of applications in materials characterization, chemical and biological sensing as well as in microfluidics. Typical biosensing applications require the use of sensors in liquid media, such as in the measurement of disease biomarkers in bodily fluids [1]. The key issues related to biosensor technology include selectivity, sensitivity, response and recovery times, detection limit, cost, and size; most of these limitations stem from biofouling resulting from the binding of undesirable moieties such as non-specific proteins to the sensor surface. Thus, removal of NSB proteins remains a challenge in biosensing applications, in addition to high device sensivity. The SAW-fluid interaction creates a pressure gradient in the direction of acoustic wave propagation in the fluid, leading to an acoustically driven streaming phenomenon known as SAW streaming [2-4] which can be used for removal of non-specifically bound (NSB) proteins in order to improve sensor selectivity and sensitivity, as has been shown experimentally [5, 6]. The efficient utilization of streaming in SAW devices requires the understanding of fluid dynamics in these systems. Coupled field fluid structure interaction models provide an alternative to experiments and can provide more detailed information about the flow field in a SAW device operating in liquid media. Thus, computational models can be used to gain insights into the acoustic streaming phenomeon which can be used for removal of NSB proteins from sensor surface to allow sensor reuse. Computational methods such as the

* Author for correspondence at email: venkat@eng.usf.edu

Campbell-Jones' method, which involve numerical solutions to equations for leaky waves or the perturbational approach are based on many simplifying assumptions [4, 7-11] and ignore the fluid mechanical properties of the fluid. These methods can be used for studying streaming in simplified geometries. Finite element models developed previously have modeled the fluid domain with the solid motion applied as a boundary condition [12]. However, to understand the SAW device interaction and fluid domain, the piezoelectric domain equations should be coupled with the fluid dynamical equations and should be solved simultaneously. Previous models have coupled the fluid and solid domains using acoustic fluid elements, which solve for the simplified Navier-Stokes equation accounting for only the pressure term in the fluid domain and ignoring viscous dissipation [13]. Such models have been used to study wave damping. A two dimensional coupled field fluid structure interaction model was developed recently [14] to investigate acoustic streaming in a SAW device based on YZ lithium niobate, in which fluid was modeled using Navier Stokes equation. Whereas such a model is appropriate for a pure Rayleigh wave such as in YZ lithium niobate, it does not provide a complete representation when the wave propagation is mixed mode and in investigating complex transducer geometries which require a full three dimensional representation. This necessitates the development of a fully coupled three dimensional FSI model of a SAW device in contact with the fluid domain. Such a model is also instrumental in investigating the effectiveness of complex transducer geometries in biofouling removal. In the present work, we have developed a 3-D coupled field FE-FSI model to investigate and analyze the streaming velocity fields in a conventional SAW device to gain insights into the acoustic streaming phenomenon and wave propagation in a device subject to liquid loading.

II. Theory

The equations governing acoustic streaming are based the general Navier-Stoke's equation for fluid flow and have been derived by Nyborg [15]

The generalized Navier Stoke's equation is written as

$$\rho\left(\frac{\partial v_f}{\partial t} + v_f \cdot \nabla v_f\right) = -\nabla P + \nabla \cdot T + f_1 \qquad (1)$$

Where ρ is the fluid density, f_1 denotes other body forces such as gravitational, v_f denotes acoustic streaming velocity, P is the pressure, and T is the deviatoric stress tensor.

The continuity equation takes the form

$$\frac{\partial \rho}{\partial t} + \nabla \cdot \rho v_f = 0 \qquad (2)$$

Also,

$$\frac{\partial\left(\rho v_f\right)}{\partial t} = \rho \frac{\partial v_f}{\partial t} + v_f \frac{\partial \rho}{\partial t} \qquad (3)$$

Combining Eqs (1) through (3),

$$\frac{\partial(\rho v_f)}{\partial t} + F = -\nabla P + \nabla \cdot T + f_1 \quad (4)$$

Where $F = \left\langle \rho v_f \cdot \nabla v_f + v_f \nabla \cdot \rho v_f \right\rangle$ (5)

F is the non linear driving force, which is the source for acoustic streaming and is related to the Reynold's stresses. <Q> represents the time average of Q to obtain a time independent quantity [16-18]. The first order velocity, required to compute the SAW induced acoustic streaming force, is calculated using the particle displacement fields generated during the propagation of a leaky SAW when the surface is in contact with a liquid [14, 18]. The force calculated using the first order velocity acts as a body force near the SAW-fluid interface. This force can be further used to compute the second order velocity, known as the acoustic streaming velocity induced by the SAW streaming force [19-21].

Coupled field FE FSI model involves the sequential solution of the piezoelectric and fluid domains and transfer of loads between the two domains as discussed in [22]

III. Computational details

In the current work, a coupled field finite element (FE) fluid-structure interaction (FSI) model of a SAW device based on YZ-$LiNbO_3$ subject to a liquid loading was developed to gain insights into the acoustic streaming phenomenon (Fig. 1). The dimensions of the piezoelectric substrate were 400µm width x 800µm propagation length x 200µm depth. Two IDT finger pairs in each port were defined at the surface. Two sets of IDTs were defined: the input IDTs and the output IDTs. The fingers were defined with periodicity of 40 µm and aperture width of 200 µm. The IDT fingers were modeled as mass-less conductors and represented by a set of nodes coupled by voltage degrees of freedom (DOF). The model was meshed with tetragonal solid elements with four degrees of freedom, three of them being the translations and the fourth being the voltage. To optimize on the computation time while capturing the interface dynamics accurately, the mesh density was such that it was refined near the fluid-structure interface and coarser away from it. A total of 2, 218, 399 nodes and 2, 085, 877 elements were generated. The equations for the piezoelectric and fluid domains were implemented and solved using Ansys® (v11.0, Ansys Inc, Canonsburg, PA).

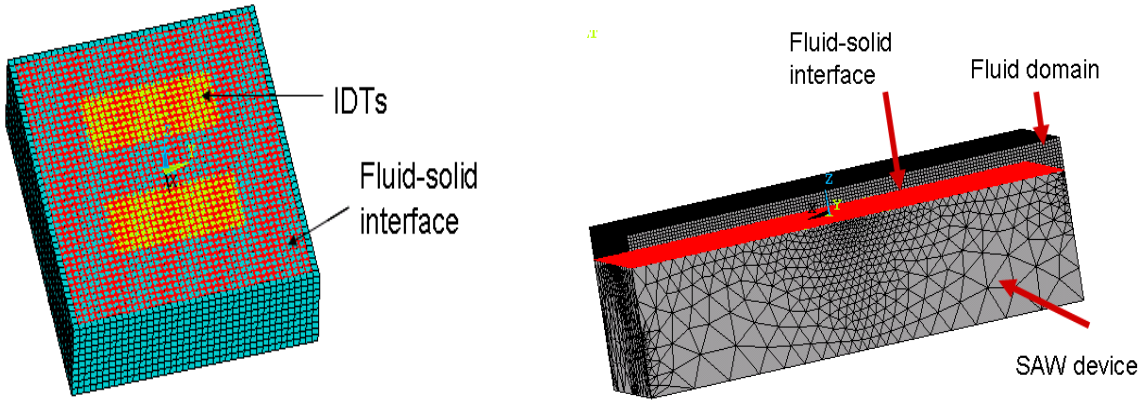

(a) (b)

Figure 1. Surface acoustic wave device **(a)** meshed structure with IDTs **(b)** fluid loading

The fluid was modeled as incompressible and Newtonian using the Navier-Stokes equation. A purely Lagrangian frame was used for the piezoelectric domain whereas mixed Lagrangian-Eulerian or Arbitrary Lagrangian Eulerian (ALE) approach was used for kinematical description of the fluid domain. To achieve bidirectional fluid structure coupling, stress and displacement continuity were maintained across the fluid-structure interface. To achieve this, displacements were transferred from solid to fluid and pressure from fluid to solid. The fluid mesh was continuously updated as the piezoelectric substrate undergoes deformation. The simulation was carried out for 100 nanoseconds (ns), with a time step of 1 ns. The excitation of the piezoelectric solid was provided by applying an AC voltage (with a peak value of 2.5 V and frequency of 100 MHz) on the input IDT fingers.

IV. Results/Discussion

The particle displacement on the SAW device, shown in Figure 3a, suggests that the maximum particle displacement occurs near the IDTs. Our simulation results indicate the particle displacement on the device decays rapidly from the surface towards the depth of the substrate as also seen in Fig. 3b.

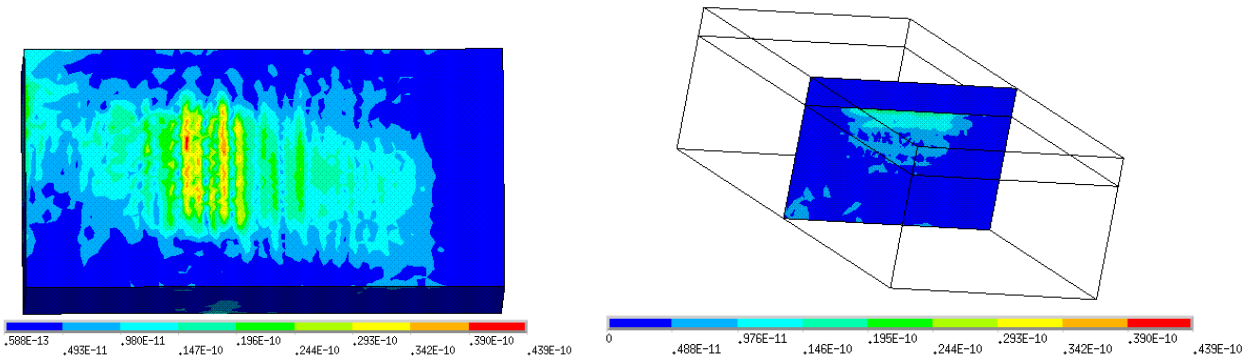

Figure 3: (a) Contours showing displacement in the piezoelectric domain of the SAW device subject to fluid loading (b) displacement profile along the depth at a section cut through the center of the delay path and normal to the propagation direction at t=70 ns.

The transient solutions generated from the model are used to predict trends in acoustic streaming velocity along various locations in a SAW delay path. The generated fluid velocity profiles in the tangential and normal directions are shown in Fig. 4a (subscripts 1 and 2 denote the propagation and transverse directions) and the total streaming velocity profile is shown in Fig. 4b. The normal component of fluid velocity is comparable to the tangential components, which is indicative of strong acoustic wave coupling with the liquid medium leading to mode conversion from Rayleigh to leaky SAW due to the launching of longitudinal waves into the liquid medium. When the intensity of these longitudinal waves is high, their attenuation leads to a net pressure gradient along the direction of wave propagation, thereby causing fluid motion. This conversion of the attenuated sound wave into flow represents the phenomenon of acoustic streaming. As evident, the fluid velocities in the SAW device are of the order of μm/s. Owing to the coupled nature of the simulation, these velocities are indicative of the device surface displacement and therefore the intensity of the longitudinal waves as well as acoustic streaming. The velocity profiles for the device indicate that the highest tangential and

normal velocities occur close to the device surface. Thus, the fluid motion is confined to the initial few fluid layers beyond which the wave motion is dampened significantly. In addition, beyond the first few layers, flow reversal is observed indicating fluid recirculation close to the SAW device surface, as also evidenced by Fig. 5.

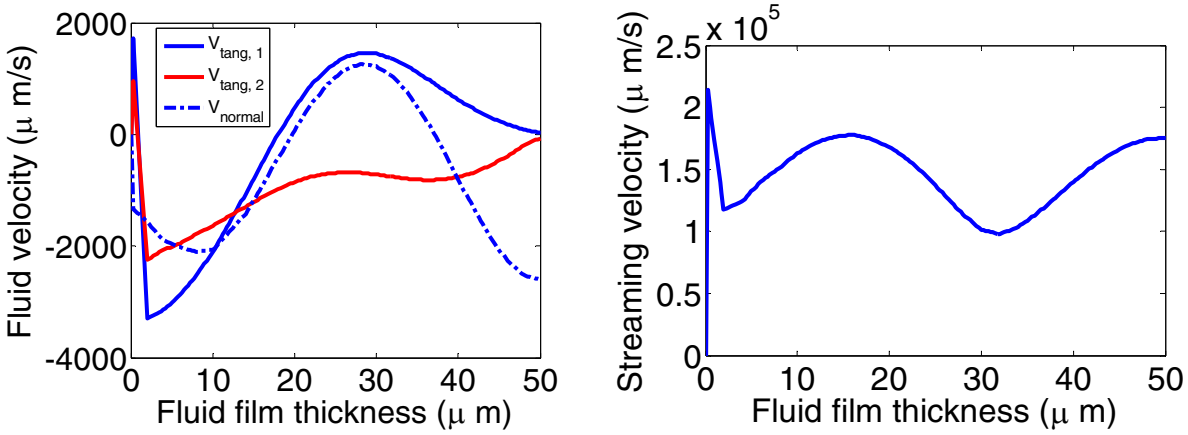

Figure 4: Fluid velocity profiles (a) velocity components in the three directions; subscripts 1 and 2 represent the propagation and transverse directions, respectively (b) total streaming velocity for the SAW device.

Whereas the tangential component of the fluid motion would lead to the advection of the biofouling proteins away from the fouled area due to drag, the normal component would prevent the readhesion of the particle from the surface by application of a lift force. Thus, both the components are important in removal of NSB proteins from the device surface. Our simulation results indicate that the magnitude of the tangential component of the SAW induced fluid velocity along the propagation direction is the highest followed by the normal component thereby suggesting that the lift forces are smaller than the drag ones and the advection of particles by the SAW induced drag force is the prominent mechanism in biofouling removal. The lift forces are important to prevent particle reattachment to the surface.

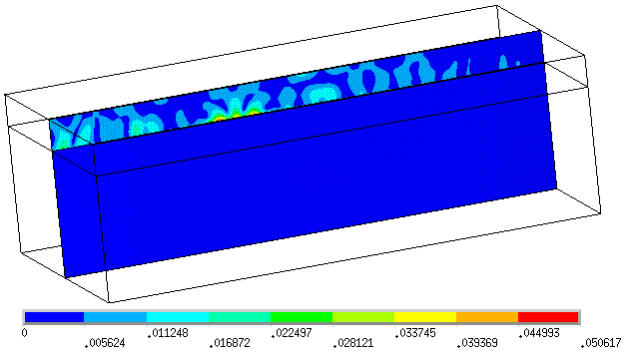

Figure 5: Fluid velocity contours on a section cut through the centre of the device along the propagation direction

The fluid velocity profiles can be used to compute the lift and drag forces on the particles which in addition to the direct SAW force and acoustic radiation force act against the

particle-surface adhesive forces and act to selectively remove the non-specifically bound proteins. A comparison of these removal forces with the adhesion forces for the specifically and non-specifically bound proteins will provide insights into mechanisms for the removal of non-specifically bound proteins from the biosensor surface. Further work is underway to compute these removal forces using the generated streaming velocity fields.

V. Conclusions

A three dimensional coupled field FE FSI model of a SAW device in contact with a fluid loading, typical of biosensing applications, was developed. The model was used to gain insights into the acoustic streaming phenomenon which can be used to remove NSB proteins from device surface thereby leading to an increased device selectivity and sensitivity towards the target analyte. Our simulation results indicate that the lift forces are smaller than the drag ones and the advection of particles by the SAW induced drag force is an important mechanism in biofouling removal. Further efforts to quantify the magnitudes of the various removal forces and compare them with the adhesive forces to predict the removal mechanism of non-specifically bound proteins from the biosensor surface are underway.

Acknowledgements

The authors gratefully acknowledge the computational resources provided by Academic computing and Engineering computing at the University of South Florida, Tampa, FL. This work was supported by NSF grants CHE-0722887 and ECCS-0801929, and IIP-07122360.

References

[1] F. Josse, F. Bender, R. W. Cernosek, et al., IEEE International Frequency Control Symposium and PDA Exhibition, 454 – 461 (2001).

[2] L. Byoung-Gook, L. Dong-Ryul, and K. Kwon, Applied physics letters **89**, 183505 (2006).

[3] K. Chono, N. Shimuzu, Y. Matsui, et al., Japanese journal of applied physics **43**, 2987 (2004).

[4] K. Chono, N. Shimizu, Y. Matsui, et al., IEEE Ultrasonics Symposium **2**, 1786 (2003).

[5] S. Cular, D. W. Branch, V. R. Bhethanabotla, et al., AIChE Annual Meeting. (2005b).

[6] S. Cular, D. W. Branch, V. R. Bhethanabotla, et al., IEEE Sensors Journal **8**, 314 (2008b).

[7] J. J. Campbell and W. R. Jones, IEEE Transactions on Sonics and Ultrasonics. **15**, 209 (1968).

[8] J. J. Campbell and W. R. Jones, IEEE Transactions on Sonics and Ultrasonics **17**, 71 (1970).

[9] L. G. Olson, Journal of of Sound and Vibration **126**, 387 (1988).

[10] T. Xue, W. Lord, and S. Udpa, IEEE Trans. Ultrason. Ferroelectr. Freq. Control. **44**, 557 (1997).

[11] T. Uchida, T. Suzuki, and S. Shiokawa, IEEE Ultrasonics symposium. **2**, 1081 (1995).

[12] N. T. Nguyen and R. M. White, IEEE Transactions on Ultrasonics, Ferroelectrics, and Frequency control **47**, 1463 (2000).

[13] S. Furukawat, T. Nomuraz, and T. Yasudaz, J. Phys. D **24**, 706 (1991).

[14] S. K. R. S. Sankaranarayanan, S. Cular, V. R. Bhethanabotla, et al., Physical Review E. **77**, 066308 (2008).

[15] W. Nyborg, *Acoustic Streaming* (Academic Press, New York, 1965)

[16] M. K. Aktas and B. Farouka, J ournal of Acoustical Society of America. **116**, 2822 (2004).

[17] S. Shiokawa, Y. Matsui, and T. Moriizumi, Japanese Journal of Applied Physics **28**, 126 (1989).

[18] S. Shiokawa, Y. Matsui, and T. Ueda, Japanese journal of applied physics **29**, 137 (1990).

[19] R. Moroney, *Ph.D. Thesis: Ultrasonic microtransport* (University of California, Berkeley, 1995)

[20] R. M. Moroney, R. M. White, and R. T. Howe, Proceedings of IEEE Ultrasonics symposium **1**, 355 (1990).

[21] R. M. Moroney, R. M. White, and R. T. Howe, Applied physics letters **59**, 774 (1991).

[22] R. Singh, S. K. R. S. Sankaranarayanan, and V. R. Bhethanabotla, AIChE Annual Meeting (2008).